



Performance of The Composite Electrode of Reduced Graphene Oxide Palm Oil Shell - Zinc Oxide (rGO_{PS} - ZnO) as a Chemical Oxygen Demand (COD) Sensor by Photoelectrocatalysis

*Thamrin Azis¹, Muhammad Z. Muzakkari¹, Muh. Nurdin¹, Maulidiyah¹, Wa O. Muslia¹, Catherina M. Bijang², & Tahril³

¹Department of Chemistry, Faculty of Mathematics and Natural Sciences, University of Halu Oleo, Kendari – Indonesia, 93232

²Chemistry Department, Faculty of Mathematics and Natural Sciences, University of Pattimura, Maluku – Indonesia, 97233

³Chemistry Education Study Program/ Department of Mathematics and Natural Science Education, Faculty of Teacher Training and Education – Tadulako University, Palu – Indonesia 94119

Received 24 March 2023, Revised 26 April 2023, Accepted 25 May 2023

doi: 10.22487/j24775185.2023.v12.i2.pp123-131

Abstract

The preparation of reduced graphene oxide composite electrodes from palm shells (rGO_{PS}-ZnO) as a chemical oxygen demand (COD) sensor by photoelectrocatalysis has been successfully carried out. The preparation of rGO_{PS} - ZnO electrodes by thermal reduction method and modified Hummer. The XRD results showed several peaks of rGO_{PS} - ZnO namely 23.287°, 26.781°, 29.889°, 32.468°, 35.109°, 37.14°, 39.822°, 43.559°, 47.927°, and 48.537°. SEM-EDX analysis reveals the surface of graphene sheets containing aggregates in the shape of small particles attached to graphene sheets. The results of the EDX analysis consisted of C 67.82%, O. 19.2%, Zn. 7.85% and 5.13% impurity. The CV and LSV tests showed that the rGO_{PS} - ZnO electrode with a variation of 1 gram: 0.3 gram had a good response to the oxidation process under visible light. The profile tests of these organic dyes (methylene blue) in concentrations of 0.5 ppm, 1.0 ppm, 2.0 ppm, and 3.0 ppm were applied by Multi Pulse Amperometry (MPA). The performance of the rGO_{PS} - ZnO electrode has been in determining the value of COD by photo electrocatalytic good sensitivity, linearity, limit of detection, repeatability, and service life. The COD value was determined using the rGO_{PS} - ZnO electrode and obtained 2.97897 mg/L O₂ close to the theoretical value.

Keywords: Cocoa shell charcoal, reduced graphene oxide (rGO), zinc oxide (ZnO), COD sensor, photo electrocatalysis

Introduction

The palm oil industry produces large amounts of industrial waste as a by-product in the form of palm shell (OPS) which contains cellulose (26.27%), hemicellulose (12.61%), and lignin (42.96%). Palm shells are solid waste from the palm oil processing industry which has a hard structure, is difficult to decompose, and has not been utilized optimally. The compound is a polymer of the element carbon which can be used as a basic material for making graphene. Graphene is an interesting material that has an unusual two - dimensional framework with a hexagonal structure of single monomolecular layers of sp² hybridized carbon atoms (Habte & Ayele, 2019) and is becoming a potential material for the development of new materials in recent decades (Tewatia et al., 2021).

The compound is a polymer of the element carbon which can be used as a basic material for making graphene. To achieve commercial value, the process of graphene oxide (GO) synthesis must be simple and cost-effective. Graphene oxide (GO) is a derivative of graphene with a layered structure (Li et al., 2021; Perdana et al., 2020; Zhounq et al., 2018). Graphene oxide (GO) can be reduced to a reduced form of GO (reduced graphene oxide, rGO). Reduced graphene oxide (rGO) has been widely developed by various researchers because of its electrical conductivity, high surface area, and thermal conductivity. Reduced graphene oxide (rGO) can be applied to electrochemical sensors (photoelectrocatalytic) in developing TiO₂ as an agent for decomposing organic matter and Chemical Oxygen Demand (COD) sensors (Azis et al., 2021).

*Correspondence:

Thamrin Azis

e-mail: thamrinazis06@gmail.com

© 2023 the Author(s) retain the copyright of this article. This article is published under the terms of the Creative Commons Attribution-NonCommercial-ShareAlike 4.0 International, which permits unrestricted non-commercial use, distribution, and reproduction in any medium, provided the original work is properly cited.

Zinc oxide (ZnO) is a semiconductor that can be used as a photocatalyst in photocatalytic reactions, especially waste treatment (Lee et al., 2016). The advantages of the ZnO catalyst are non-corrosive, environmentally friendly, high dielectric constant, relatively abundant, stable, non-toxic, bandgap energy of 3.37 eV, and excitation energy of 60 meV. The large band gap energy makes ZnO only active by exposure to UV light thereby limiting its performance. The limitations of the ZnO photocatalyst can be overcome by modifying (doping) the ZnO material using reduced graphene oxide (rGO). Based on this background, research was conducted on the performance of reduced graphene oxide composite electrode palm oil shell zinc oxide (rGOAK - ZnO) as a chemical oxygen demand (COD) sensor by photoelectrocatalysis.

Methods

Instruments and materials

X-Ray Diffraction (Shimadzu 6000), Fourier Transform InfraRed (FTIR), (Shimadzu 8400), Scanning Electron Microscope - Energy Dispersive X-Ray (SEM - EDX) (HITACHI SU 3500), UV - Vis spectrophotometer (UVD - 2950, Labimed, INC). The materials used are potassium permanganate (KMnO_4) (Merck), sulfuric acid (H_2SO_4) (Merck), hydrogen peroxide (H_2O_2) (Merck), hydrochloric acid (HCl) (Merck), Methylene Blue, Whatman filter paper, aluminum foil, liquid paraffin, sodium nitrate (NaNO_3), and ZnO powder.

Synthesis of graphite oxide

The method used to oxidize graphite to graphite oxide in this study is the modification of Hummer's Method. Synthesis begins with stirring 2 grams of palm shell graphite, and 4 grams of NaNO_3 graphite with 98 ml of 98% H_2SO_4 for 4 hours in an ice bath at a temperature of around 5 °C. After that, 8 grams of KMnO_4 were added gradually for one hour. The solution was removed from the ice bath and stirred at 25 °C for 20 hours. After that, the addition of 200 ml of distilled water was carried out in stages. After 1 hour of stirring, 30 % H_2O_2 was added to the solution. The addition of H_2O_2 aims to stop the oxidation process and cause the color of the solution to turn yellow. The solution was left in a stirring condition for 30 minutes, then the solution was centrifuged to separate the precipitate. After that, 15 mL of 37% HCl was added to remove the remaining metal ion. Then it periodically washed until neutral pH is was obtained. During the washing process, the color of the solution would turn darker due to the peeling of graphite to graphite oxide. The neutral solution was then dried at 105 °C for 12 hours to obtain a graphite oxide sheet.

Preparation of rGOAK-ZnO electrodes

The rGOAK-ZnO powder with mass variations of 0.1 grams, 0.2 grams, and 0.3 grams of ZnO was crushed and put into a watch glass containing paraffin. Then, heated to a paraffin temperature of 80 °C. The mixture is stirred and inserted into the electrode body while being pressed so that it solidifies. The composite material was characterized using SEM-EDX, XRD, and FTIR.

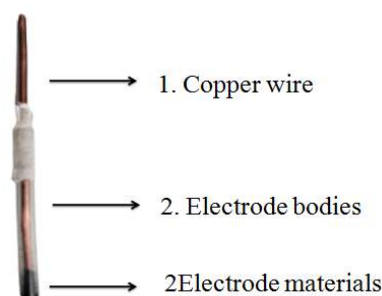


Figure 1. The working electrode components.

Characterization of rGOAK - ZnO composites

To assess the characteristics of ZnO/rGO / TiO_2 composite. To determine the crystal structure. Analysis using XRD was carried out to determine the crystal structure of graphene which had been synthesized at an angle of $2\theta^0 = 20 - 80^0$ and $\lambda \text{ Cu} - \text{K}\alpha = 1.54060 \text{ \AA}$. Fourier Transform Infrared Spectroscopy (FTIR) (Scientific Nicolet iS10) test was done to determine the functional groups of the composite at the wavenumber range $4000 - 400 \text{ cm}^{-1}$.

Measurement of chemical oxygen demand (COD)

Measurement of COD using photoelectrocatalysis is based on the photocatalytic reaction that occurs on the surface of ZnO. Photoelectrocatalysis with e^-/h^+ photogeneration pairs play a role in the reduction-oxidation reactions of organic compounds in solution. When the electrode is irradiated with UV light, the decomposed substance will release electrons. Then transferred to the working electrode. The electrons produced in the form of a light current are used as

an amperometric analytical signal. The light current will decrease until the rate of oxidation is equal to the rate of diffusion so that the current value is zero when the light is turned off. The COD value is determined by the following equation.

$$[\text{COD}]_{\text{theoretic}} = \frac{Q}{4FV} \times 32000 \quad (1)$$

$$[\text{COD}]_{\text{theoretic}} = 8000nC \quad (2)$$

where

Q = the charge (Coulomb)

I = light current

A = the number of electrons transferred

F = Faraday constant

V = the sample volume

C = the concentration (Molar)

Results and Discussion

Synthesis of reduced graphene oxide of palm shells

Graphite palm shell charcoal is oxidized to graphite oxide using a NaNO_3 catalyst, H_2SO_4 solvent, and KMnO_4 oxide. In the synthesis process, Oxidation using KMnO_4 aims to weaken the distance between the layers to facilitate the exfoliation process of graphite oxide into graphene oxide (Yusoff et al., 2017; Elfaham et al., 2021; Jain et al., 2022). Furthermore, the graphene oxide (GO) solution was heated using a hydrothermal apparatus to form a more stable GO structure. From this reduction process *reduced graphene oxide* (rGO) material will be formed (Rattan et al., 2020; Jose et al., 2018), as shown in Figure 2.

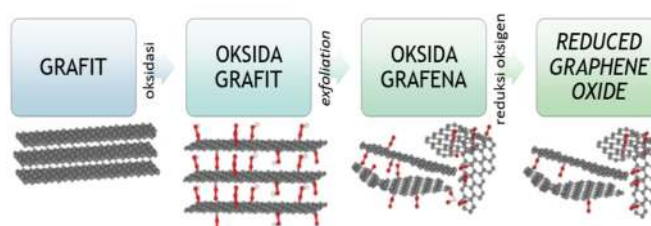


Figure 2. Preparation of reduced graphene oxide (rGO).

Characterization of fourier transform infrared (FTIR)

The characterization results of GO_{PS} , rGO_{PS} , and $\text{rGO}_{\text{PS}} \text{ZnO}$ with Fourier Transform Infrared (FTIR) can be shown in Figure 3. Figure 3 shows the FTIR spectra of the GO, and $\text{ZnO} - \text{rGO}_{\text{PS}}$ composites. In the FTIR spectrum for GO, the broad peak centered at 3423 cm^{-1} is attributed to the O-H stretching vibrations, and the peaks at 2924

cm^{-1} , 1712 cm^{-1} , 1589 cm^{-1} , 1028 cm^{-1} and 1587 cm^{-1} are assigned to the C-H, C=O sp^2 -hybridized C=C group and C-O stretching, respectively. In contrast, the peaks at 2924 cm^{-1} , 1712 cm^{-1} , 1589 cm^{-1} , and 1028 cm^{-1} are missing from the FTIR spectra of the $\text{ZnO} - \text{rGO}_{\text{PS}}$ composites. In addition, the $\text{ZnO} - \text{rGO}_{\text{PS}}$ FTIR spectra showed a peak at 712 cm^{-1} where ZnO bonds identified ZnO compounds.

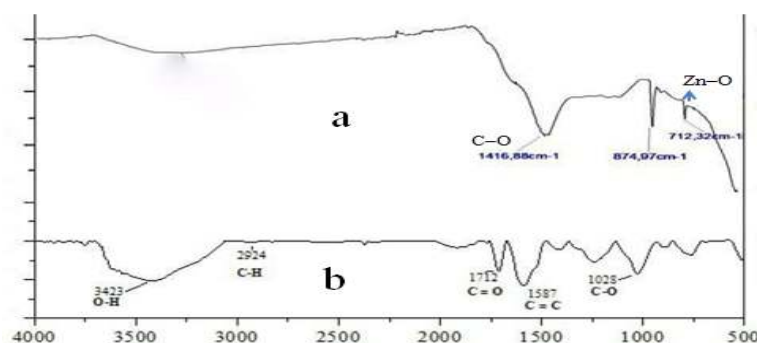


Figure 3. FTIR spectra of the GO, rGO_{PS} , and $\text{ZnO} - \text{rGO}_{\text{PS}}$ composites.

X-Ray diffraction (XRD)

Characterization was performed using XRD to determine the crystal structure of the $\text{rGO}_{\text{PS}} - \text{ZnO}$ composite electrode. The x-ray diffraction pattern shows specific peaks which are characteristic of $\text{rGO}_{\text{PS}} - \text{ZnO}$. The XRD patterns of the obtained products are shown in Figure 4. Figure 4 showed the results of the graphene oxide (GO) $\text{rGO}_{\text{PS}} - \text{ZnO}$ pattern. Based on the results, it can be a ractogram for peaks of $2\theta = 12.39^\circ$ (d - spacing = 7.138 \AA), 26.7° (d - spacing = 7.138 \AA), and 44.04°

(d - spacing = 3.350 \AA). The characteristic feature of GO crystals is that they have 2θ bands at 25° and 45° (Putri et al., 2019; Robaiah et al., 2019). The observed peak confirms that the graphene oxide sheet peels off from the graphite flakes. In addition, the $\text{rGO}_{\text{PS}} - \text{ZnO}$ diffraction pattern indicated several peaks at an angle of 2θ , namely 23.287° (d - spacing = 3.350 \AA), 26.781° (d - spacing = 3.34976 \AA), 29.889° (d - spacing = 3.03552 \AA), 32.468° (d - spacing = 2.8181 \AA), 32.468° (d - spacing = 2.6038 \AA), 35.109° (d - spacing = 2.49305 \AA), 37.14° (d - spacing = $2, 28422 \text{ \AA}$), 39.822° (d - spacing =

2.09428 Å), 43.559° (d - spacing = 2.09428 Å), 47.927° (d - spacing = 1.91183 Å) and 48.537° (d - spacing = 1.87479 Å) (Liu et al., 2018).

From the data, showing doped rGO_{PS} in ZnO, it is proven that there are peaks of rGO_{PS} and ZnO crystals in the obtained XRD diffractogram

pattern. Based on standard joint committee powder of diffraction ZnO (JCPDS 36 - 1451), The results of the XRD characterization show that ZnO has a distinctive peak at an angle of 2θ = 35.109°, 37.14° (100), 39.822° (101); 47.927 ° and 48.537 ° (102).

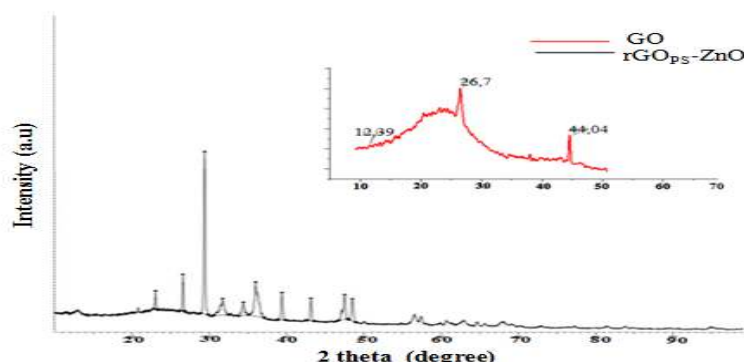


Figure 4. XRD patterns of GO and rGO_{PS}- ZnO.

SEM and EDX

The morphology of the rGO_{PS}- ZnO sample at the ×5000 and ×10000 magnification is shown in Figure 5. Figure 5 is the result of SEM characterization of the rGO_{PS}- ZnO composite, showing the morphology of the porous surface

containing bright black and white particles identifying the presence of rGO_{PS} and ZnO particles.

The EDX analysis results are shown in Figure 6. Showed the presence of carbon (C), oxygen (O), and zinc (Zn) elements to identify the success of doping rGO_{PS} on ZnO.

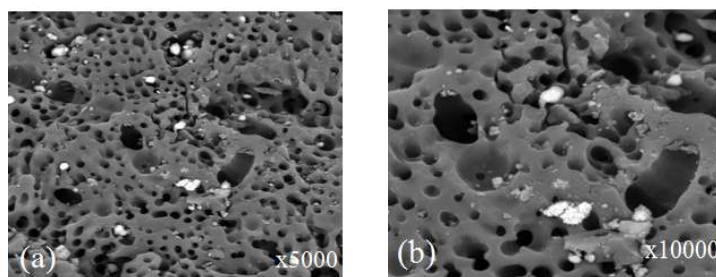


Figure 5. Morphology of rGO_{PS}- ZnO (a) Magnification ×5,000 and (b) ×20,000.

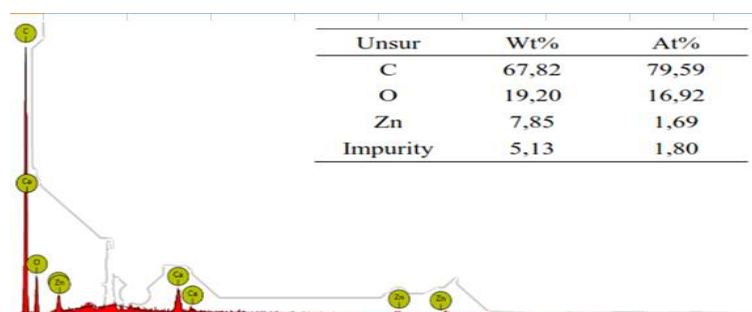


Figure 6. EDX result of ZnO.

Activity test of rGO_{PS}- ZnO electrode using LSV and CV

The electrochemical test has applied using three electrodes variation namely rGO_{PS}- ZnO, platinum (Pt) electrode, and Ag/AgCl electrode. The electrolyte was used at 0.01 M K₃[Fe(CN)₆] to

observe the reduction–oxidation (redox) peaks and also the rate of electron transfer (Momeni et al., 2019).

Figure 7 shows the voltammogram curve of the K₃[Fe(CN)₆] electrolyte using a scan rate of 1,0 Vs⁻¹ in the potential range from - 0.8 to 0.8 Vs⁻¹.

The high intensity of the current peak from the four electrodes was measured regarding redox peaks (I_{pa} = oxidation current; I_{pc} = reduction current; E_{pa} =

oxidation potential; E_{pc} = reduction potential), which can be seen in **Table 1**.

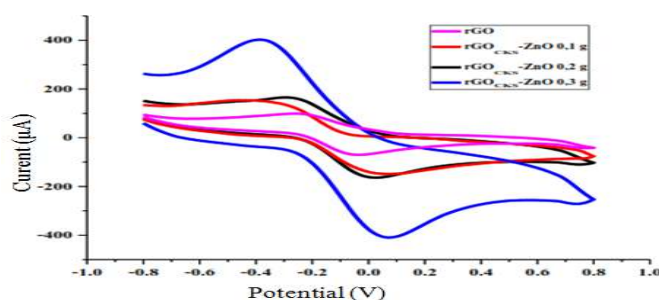


Figure 7. The CV graph comparing the four working electrodes using $K_3[Fe(CN)_6]$ as the electrolyte solution

Table 1. The three working electrodes' performance regarding oxidation–reduction peak (refers to **Figure 7**).

Electrode	$I_{pa}(\mu A)$	$I_{pc}(\mu A)$	$E_{pa}(V)$	$E_{pc}(V)$
rGO _{PS}	49	-19	-0,24	-0,04
rGOCKS - ZnO 0,1 g	95	-30	-0,29	0,01
rGOCKS - ZnO 0,2 g	102	-48	-0,36	0,02
rGOCKS - ZnO 0,3 g	226	-92	-0,39	0,06

Based on **Figure 7** and **Table 1** shows the measurements using the four electrodes under $K_3[Fe(CN)_6]$ electrolyte solution have produced the redox peaks with a scan rate of $1,0 \text{ Vs}^{-1}$. The 0.3 g rGOCKS-ZnO electrode gave a higher peak current response ($266 \mu A$) compared to other electrodes. This is due to an increase in the number of electron transfers from the analytes produced from doping.

The Linear Sweep Voltammetry (LSV) method is a micro-scale electroanalytic method that

examines information about the analyte based on the measurement of current (I) as a function of potential (V) using $0.1 \text{ M } K_3[Fe(CN)_6]$ electrolyte solution connected to the Portable Potentiostat (Azis et al., 2021), measurement of the response of the photocurrent (light current) which is the current that can be observed when the electrode is irradiated with UV and Visible light.

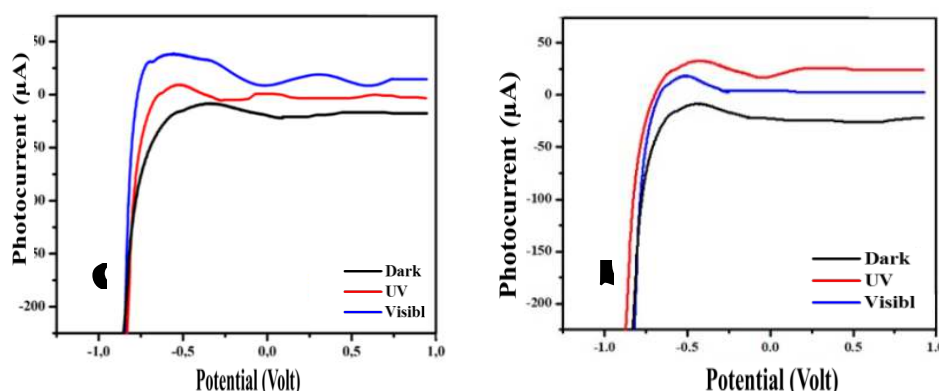


Figure 8. Test of electrode activities by the process of LSV (a) ZnO and (b). rGO_{PS} – ZnO.

The light current response of the electrode that is not illuminated by UV light (dark) does not indicate a light current. This is because electrons and holes are not formed as the initiator of oxidation and reduction reactions. When the UV illumination of ZnO and (b). rGO_{PS} - ZnO electrodes show a high increase in light current, this indicates photocatalytic activity.

Figure 8a shows that when hit UV light irradiation, ZnO electrode performance is higher. This is consistent with the theory that TiO_2 is active with an energy gap of 3.2 eV only in the UV region with a wavelength of around 388 nm (Maulidiyah, et al., 2017). **Figure 8b** shows the effect of UV light irradiation, visible light, and not irradiation (dark) on the rGO_{PS} - ZnO working electrode. When the

rGO_{PS} - ZnO electrode is irradiated with visible light, it shows an increase in the light current. This is because rGO_{PS} doping has decreased ZnO bandgap energy and serves as an electron acceptor to increase the electrons and holes that enter the ZnO surface. On the other hand, the addition of rGOPS dopant to ZnO can reduce the energy gap of ZnO, so that the electrodes can absorb light at a fairly large wavelength with less energy (Basavarajappa et al., 2020).

Photocurrent response of the methylene blue

Photocurrent response measurement of ZnO electrodes and rGO_{PS} - ZnO electrodes to Methylene Blue was carried out using the Multi Pulse Amperometry (MPA) method. The test was carried out on the test solution with respective concentrations of 0.5, 1, 2, and 3 ppm. The amperogram of rGO_{PS} - ZnO electrode again methylene blue is shown in Figure 9.

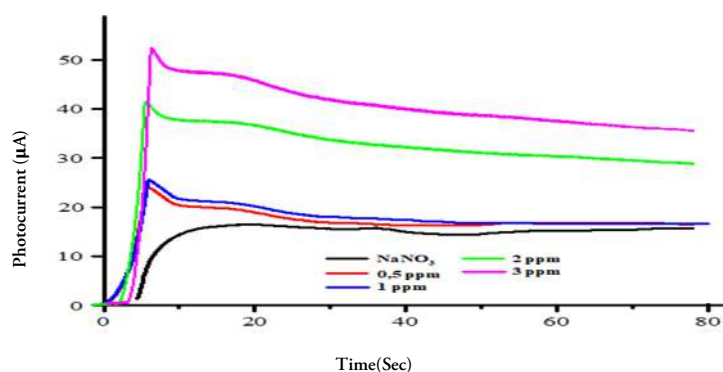


Figure 9. The photocurrent response of methylene blue, amperogram of rGO_{PS} - ZnO electrode

Figure 9 shows the photocurrent produced by methylene blue (MB) is greater than that of the electrolyte solution. The resulting light current is the sum of the oxidation currents of methylene blue (MB) and the oxidation currents of electrolyte solutions. The photocurrent produced by methylene blue (MB) is greater than that of the electrolyte solution. The decrease in photocurrent occurs because the methylene blue (MB) compound

decreases in solution due to photocatalytic degradation. The greater the concentration of organic compounds, the higher the photocurrent response produced.

The performance of the rGO_{PS} - ZnO electrode is known by observing the proximity of the generated charge value to the theoretically generated charge value. Figure 10 shows Q_{net}'s relationship with methylene blue (MB) compounds.

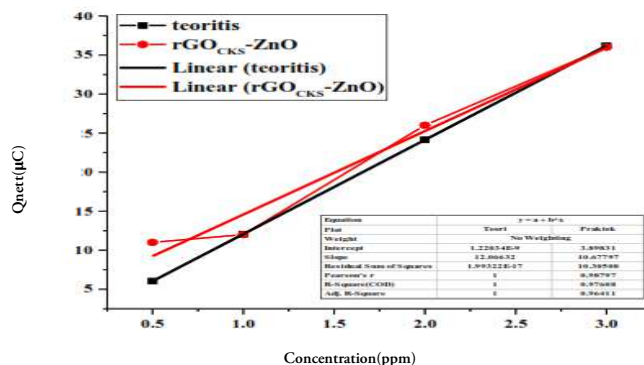


Figure 10. The relation between Q_{net} and concentration of methylene blue (MB) compound.

Based on Figure 10 the performance of the rGO_{PS} - ZnO electrode shows the highest level of accuracy in methylene blue (MB). This is due to the molecular structure of methylene blue (MB) which makes it easy to mineralize. In addition, the resulting charge is directly related to the concentration of the test compound. This is in line with the law of Faraday, which states that the greater the solution concentration, the greater the charge received. This is due to the interaction of the analyte molecule and the surface of the electrode. The

strong interaction with the surface of the catalyst causes an increase in the rate of oxidation of organic compounds so that the resulting load is greater.

Determination of chemical oxygen demand (COD) value

Figure 11 represents the linearity of the measurement data for COD values on methylene blue (MB) using the rGO_{PS} - ZnO electrode to see the theoretical COD value with a photo electrocatalytic approach.

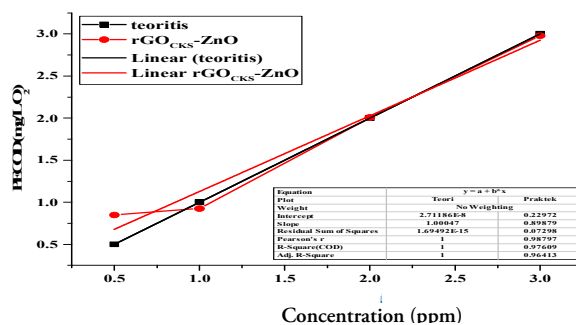


Figure 11. The relation between COD PEC and concentration of methylene blue (MB) compound

Figure 11 compares theoretical COD values and COD PEC values as the methylene blue (MB) concentration increases from 0.5 ppm to 3.0 ppm. The data show that increasing the concentration of methylene blue (MB) makes the COD PEC value

close to linearity to the theoretical COD value so that the probability of linearity is observed at methylene blue (MB) concentrations from 0.5 ppm to 3.0 ppm, as shown in Table 2.

Table 2. Methylene blue (MB) COD using rGO_{PS} - ZnO electrode

Concentration (ppm)	COD (mg/L O ₂)	
	Theoretical	Photoelectrocatalytic (COD PEC)
0.5	0.5002345	0.84907
1.0	1.000469	0.92626
2.0	2.0009379	2.00689
3.0	3.0014069	2.97877

Determination of linearity, detection limit, and sensitivity

The linear regression equation applied to the results must have intercept values not significantly

different from zero. If the non-zero significant intercept is obtained, it must be proved that this does not affect the accuracy of the method (Veerasingam et al., 2011).

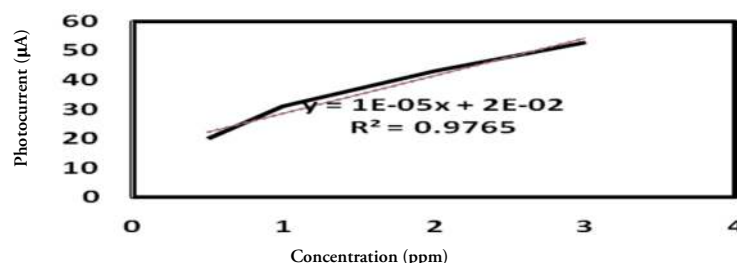


Figure 12. Linear graph of methylene blue test compound

The linearity can be found from the coefficient slope based on methylene blue concentration toward the oxidation peak (I_p value) which showed in Figure 12. We obtain the linearity equation $y = 10^{-5}x + 0.02$ with an intercept value of 0.02 and a slope of 10^{-5} . It aims to determine the range area that occurs in measuring the methylene blue compound by $R^2 = 0.9765$ or close to 1. At low concentrations, the photodegradation process is only influenced by the photo hole capture process on the catalyst surface while at high concentrations compound structures affect the photodegradation process of the compounds (Muzakkar et al., 2021).

Determination of the detection limit was carried out to find out the smallest concentration of methylene blue in the sample that can still be detected by the rGOAK - ZnO sensor and still

provide a significant response. Detection limit shows the level the sensitivity of the electrode, the lower the detection limit, the better its sensitivity to the sample (Lukmana & Setiarso, 2018). Then, the LoD has been obtained from calculation results is 0.06 ppm which shows that rGO_{PS} - ZnO composite can detect methylene blue compound up to a concentration of 0.06 ppm. The rGOAK - ZnO electrode has the capability of detecting methylene blue with high sensitivity. This can be seen from the greater slope and higher sensitivity.

Electrode repeat test

The repeatability test was conducted to exhibit the working electrode performance against the consistency of measurement. This treatment of the rGOAK - ZnO composites has been tested by

using methylene blue. **Figure 13** depicts the results of the repeatability working electrode that the high-performance.

Figure 13 depicts the results of the repeatability working electrode that the high-performance of rGO_{PS} - ZnO stability for 15 times

tested. Based on this study **Figure 13**, we obtain calculated the standard deviation (SD) of 1.57 and Relative Standard Deviation (RSD) is 2.48%. We declare that the rGO_{PS} - ZnO composites have stabilized due to the Horwitz value obtained less than 2% (1.24%).

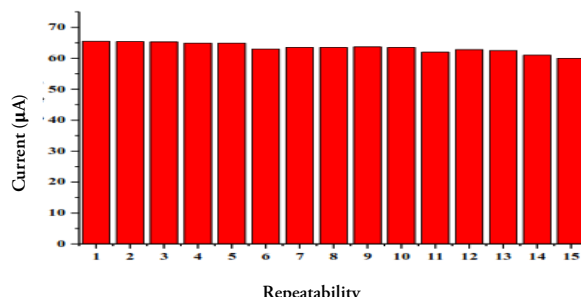


Figure 13. The histogram of oxidation current versus the repeating measurement

Electrode lifetime determination

Especially, we explore a lifetime of rGO_{PS} - ZnO to obtain the high-performance electrode for 14 days. The lifetime test performance has been carried out by using the same solution on the

repeatability test extension lifetime electrode enforced for clarifying rGO_{PS} - ZnO to sensitivity against fipronil. to sensitivity against methylene blue. Meanwhile, if it is to be increased, the rGO_{PS} - ZnO composite must remove organic compounds on the surface of the electrode.

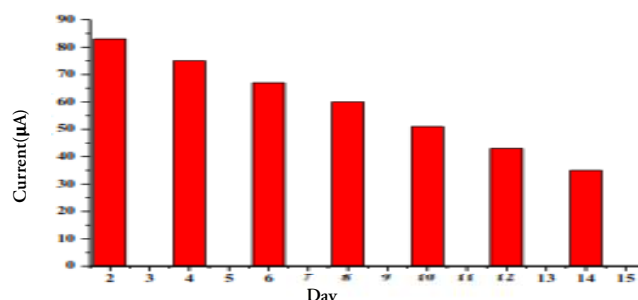


Figure 14. lifetime test of rGO_{PS} - ZnO composites

Figure 14 exhibits that the optimum performance electrode from 1 to 8 days is relatively stable, while the 9 to 14 days is the low-performance electrode. This condition that the longer electrode used causes thickening diffusion on the electron transfer system and limits peak current.

Conclusion

Electrodes of rGO_{PS}-ZnO have been successful. Then the rGO_{PS}-ZnO electrodes were characterized using FTIR, XRD, and SEM-EDX. FTIR results show absorption at wavenumbers of 1416 cm⁻¹ and 712 cm⁻¹, indicated as C-O and Zn-O bonds. The XRD results of rGO_{PS}-ZnO show peaks at an angle of 2θ, namely 23.287°, 26.781°, 29.889°, 32.468°, 35.109°, 37.14°, 39.822°, 43.559°, 47.927°, and 48.537°. SEM-EDX analysis revealed a porous graphene sheet surface and black and white colored particles identified the presence of rGO and ZnO. The results of the EDX analysis consisted of C 67.82%, O. 19.20%, Zn. 7.85% and 5.13% impurity. The detection limit obtained was

0.06 ppm. and the repeatability was indicated by a Horwitz Ratio (HorRat) value of 1.24%. The optimum measurement stability in analyzing methylene blue is 14 days. The COD value is close to the theoretical concentration of 3 ppm (2.97897 mg/L O₂).

Acknowledgments

The authors would like to thank the Physical Chemistry Laboratory and the Inorganic Laboratory of the Faculty of Mathematics and Natural Sciences, Halu Oleo University, which have assisted in completing this research.

References

Azis, T., Maulidiyah, N., Muzakkar, M. Z., Ratna, R., Kadir, L. O., Islami, M., Nurwahida, T., Bijang, C. M., & Nurdin, M. (2021). Tellurium (Te-TiO₂/Ti) doped TiO₂/Ti composite synthesis for degradation of reactive blue 160 by photoelectrocatalysis. *Technology Reports of Kansai University*, 63(5), 7611-7621.

- Basavarajappa, P. S., Patil, S. B., Ganganagappa, N., Reddy, K. R., Raghu, A. V., & Reddy, C. V. (2020). Recent progress in metal-doped TiO₂, non-metal doped/codoped TiO₂ and TiO₂ nanostructured hybrids for enhanced photocatalysis. *International Journal of Hydrogen Energy*, 45(13), 7764-7778.
- ElFaham, M. M., Mostafa, A. M., & Mwafy, E. A. (2021). The effect of reaction temperature on structural, optical and electrical properties of tunable ZnO nanoparticles synthesized by hydrothermal method. *Journal of Physics and Chemistry of Solids*, 154(July), 1-8.
- Habte, A. T., & Ayele, D. W. (2019). Synthesis and characterization of reduced graphene oxide (rGO) started from graphene oxide (GO) using the tour method with different parameters. *Advances in Materials Science and Engineering*, 2019(August), 1-9.
- Jain, N., Sharma, S., & Puri, N. K. (2022). Investigation of charge transport mechanism in hydrothermally synthesized reduced graphene oxide (rGO) incorporated zinc oxide (ZnO) nanocomposite films. *Journal of Materials Science: Materials in Electronics*, 33(January), 1307-1323.
- Jose, P. P. A., Kala, M. S., Kalarikkal, N., & Thomas, S. (2018). Reduced graphene oxide produced by chemical and hydrothermal methods. *Materialstoday: Proceedings*, 5(8), 16306-16312.
- Lee, K. M., Lai, C. W., Ngai, K. S., & Juan, J. C. (2016). Recent developments of zinc oxide based photocatalyst in water treatment technology: A review. *Water Research*, 88(January), 428-448.
- Li, Q., Ding, Y., Yang, L., Li, L., & Wang, Y. (2021). Periodic nanopatterning and reduction graphene oxide by femtosecond laser to construct high-performance micro-supercapacitors. *Carbon*, 172(October), 144-153.
- Liu, C., Yue, M., Liu, L., Rui, Y., & Cui, W. (2018). A separation-free 3D network ZnO/rGO-rGH hydrogel: Adsorption enriched photocatalysis for environmental applications. *Royal Society of Chemistry Advances*, 8(40), 22402-22410.
- Lukmana, K. M., & Setiarso, P. (2018). Pembuatan elektroda kerja graphene oxide untuk analisis parasetamol secara siklik voltametri. *UNESA Journal of Chemistry*, 7(02), 58-63.
- Maulidiyah., Azis, T., Nurwahidah A. T., Wibowo, D., & Nurdin, M. (2017). Photoelectrocatalyst of Fe co-doped N-TiO₂/Ti nanotubes: Pesticide degradation of thiamethoxam under UV-visible lights. *Environmental Nanotechnology, Monitoring & Management*, 8(December), 103-111.
- Momeni, M. M., & Mahvari, M., & Ghayeb, Y. (2019). Photoelectrochemical properties of iron-cobalt WTiO₂ nanotube photoanodes for water splitting and photocathodic protection of stainless steel. *Journal of Electroanalytical Chemistry*, 832(January), 7-23.
- Muzakkar, M. Z., Natsir, M., Alisa, A., Maulidiyah, M., Salim, L. O. A., Sulistiyan, I., Mustapa, F., Ratna., & Nurdin, M. (2021). Photoelectrocatalytic degradation of reactive red 141 using FeTiO₃ composite doped TiO₂/Ti electrodes. *Journal of Physics: Conference Series* (pp. 1-9). United Kingdom: IOP Publishing Ltd.
- Perdana, Y. A., Joni, R., Emriadi., & Aziz, H. (2020). Effect of KOH activator on the performance of activated carbon from oil palm kernel shell as supercapacitor electrode material. *Journal of Aceh Physics Society*, 9(1), 13-19.
- Putri, N. P., Kusumawati, D. H., Agustina, L., & Munasir. (2019). Effect of calcination temperature on characteristics of reduced graphene oxide (rGO) made from old coconut shell. *IOP Conference Series: Journal of Physics: Conference Series* (pp. 1-6). United Kingdom: IOP Publishing Ltd.
- Rattan, S., Kumar, S., & Goswamy, J. K. (2020). Graphene oxide reduction using green chemistry. *Materialstoday: Proceedings*, 26(September), 3327-3331.
- Robaiah, M., Mahmud, M. A., Salifairus, M. J., Khusaimi, Z., Azhan, H., Abdullah, S., Rusop, M., & Asli, N. A. (2019). Synthesis and characterization of graphene from waste cooking palm oil at different deposition temperatures. *AIP Conference Proceedings* (pp. 020026-1- 020026-6). USA: AIP Publishing.
- Tewatia, K., Sharma, A., Sharma, M., & Kumar, A. (2021). Synthesis of graphene oxide and its reduction by green reducing agent. *Materialstoday: Proceedings*, 44(September), 3933-3938.
- Veerasamy, R., Rajak, H., Jain, A., Sivadasan, S., Varghese, C. P., & Agrawal, R. K. (2011). Validation of QSAR models - strategies and importance. *International Journal of Drug Design and Discovery*, 2(3), 511-519.
- Yusoff, N., Rameshkumar, P., Mehmood, M. S., Pandikumar, A., Lee, H. W., & Huang, N. M. (2017). Ternary nanohybrid of reduced graphene oxide-nafio@silver nanoparticles for boosting the sensor performance in non-enzymatic amperometric detection hydrogen peroxide. *Biosensors and Bioelectronic*, 87(January), 1020-1028.
- Zhoung, M., Zhang, F., Yu, Y., Zhang, J., Shen, W., & Guo, S. (2018). Flexible micro-supercapacitors assembled via chemically reduced graphene oxide films assisted by laser printer. *Nanotechnology*, 29(43), 1-7.